Postprint of: Litzbarski L., Winiarski M., Skokowski P., Klimczuk T., Andrzejewski B., Investigation of magnetic order in a new intermetallic compound Nd_2PtGe_3, JOURNAL OF MAGNETISM AND MAGNETIC MATERIALS, Vol. 521, iss. Part 1 (2021), 167494, DOI: 10.1016/j.jmmm.2020.167494

Investigation of magnetic order in a new intermetallic compound Nd_2PtGe_3

L.S. Litzbarski[a,b], M.J. Winiarski[a,b], P. Skokowski[c], T. Klimczuk[a,b], B. Andrzejewski[c]

[a] *Faculty of Applied Physics and Mathematics, Gdansk University of Technology,*

Narutowicza 11/12, 80-233 Gdansk, Poland

[b]*Advanced Materials Centre, Gdansk University of Technology,*

ul. Narutowicza 11/12, 80-233 Gdańsk, Poland,

[c] *Institute of Molecular Physics, Polish Academy of Science,*

Smoluchowskiego 17, 60-179 Poznan, Poland

Abstract

In the present study we report a successful synthesis of the new intermetallic compound Nd_2PtGe_3 by an arc-melting method. The powder X-ray diffraction analysis indicates that this compound crystallizes in an disordered variant of the AlB_2-type structure (space group P6/mmm, no. 191) with lattice parameters a = 4.2455 Å and c = 4. 1933 Å. The compound exhibits a cluster-glass transition below T_f = 2.9 K, characterized through ac and dc magnetic susceptibility and heat capacity measurements.

Introduction

According to conventional definition, spin glasses are family of random magnets, in which ferromagnetic and antiferromagnetic spin-spin interactions exist simultaneously and compete, leading to ordering frustration (see for example the handbook of Kawamura [1]). In this type of systems, spins are arranged quasi-randomly and exhibit no long-range periodicity.

Spin glass systems can be very diverse from the point of view of structure and chemical composition and can be represented, for example, by such different chemical compounds like alloys U_2NiSi_3 [2], $CeCu_4Mn_yAl_{1-y}$ [3] or oxides $BaBi_{0.28}Co_{0.72}O_{2.2}$ [4], but all of them have common properties, like: magnetic frustration due to competing interactions, and site disorder [5]. Magnetic disorder of spin glasses becomes frozen under the critical temperature called freezing temperature T_f, but unlike for

ordered systems it can slowly evolve with time to attain local energy minimum. Below freezing temperature spin glass systems exhibit also some magnetic irreversibility.

For example, superparamagnetic (SP) and superferromagnetic (SFM) systems or ferromagnets (FM) with domain walls can also exhibit magnetic relaxation, aging, rejuvenation and memory effect and sometimes also the existence of de Almeida-Thouless line (AT-line) [6]. Magnetic relaxation in SFM or FM systems can be driven, among others, by growth or reorientations of magnetic domains controlled by wall pinning on structural defects, grain boundaries and motion of domain walls which makes time evolution of their magnetization very complex. Spin glasses, however, can be distinguished from magnetically ordered systems due to their specific form of magnetization relaxation. The Arrot plot can be also helpful because it allows confirming (or excluding) magnetic ordering.

The time evolution of the magnetic moment due to domain reorientation is usually described by modified power law model: $m(\tau)=m_0+m_r\tau^{n-1}$ where τ is normalized time $\tau=t/t_0$, m_0 is initial magnetization and m_r relaxing component of magnetization. Magnetic relaxation in SFM domain system, obeys stretched exponential law $m(\tau)=m_0+m_r[1-\exp(-\tau/\tau_0)^{\beta}]$. However, this model also correctly describes relaxation in the spin-glass and in spin cluster glass systems with properties determined by multiple spin interactions rather than individual spins. The unique magnetic relaxation corresponding to spin-glass state is represented by logarithmic dependence: $m(t) = m_0 + S\ln(t/t_0 + 1)$, where m_0 and S are magnetization at $t = 0$ and the magnetic viscosity, respectively. The above examples show that magnetic relaxation measurements are crucial for studying and understanding the spin-glass state phenomena.

In addition to experimental studies, modeling of spin glasses has also a large influence on development of new algorithms for solving many combinatorial optimization problems i.e. the Traveling Salesman Problem, airline scheduling, pattern recognition and circuit wiring [7].

Ternary intermetallic R_2TX_3- type family, where R means rare-earth ions, T is a transition metal and X = Si, Ge, Ga, In, is an attractive system to investigate compounds with intriguing physical properties. These compounds generally crystalize in AlB_2 – derived crystal structure with space group *P6/mmm*, which exist both in disordered and ordered variant [8]. In the crystal lattice of disordered R_2TX_3 compounds R ions occupy Wyckoff 1*a* site, forming hexagonal lattice, while T and X are randomly distributed in honeycomb layers, as shown in Fig 1 (all crystal structure drawings were generated using the VESTA program [9]). The statistical distribution of T and X atoms cause a varying environment around R ions, which leads to the magnetic cluster formation. Moreover, the c/a ratio is about 1 which suggests that the strength of nearest-neighbor exchange (NN) and next-nearest-neighbor exchange (NNN) interactions are comparable, which may promote existence of magnetic frustration [10]. For these reasons many of R_2TX_3 compounds exhibit glassy behavior i.e. $Sm_2Ni_{0.87}Si_{2.87}$ [11],

$Tb_2N_{0.90}Si_{2.94}$ [12] and $Nd_2Ni_{0.94}Si_{2.94}$ [13] are cluster-glasses, while Gd_2NiSi_3 [14] and Nd_2PdSi_3 [15] were identified as canonical spin-glasses.

In this paper, we report successful synthesis of a novel intermetallic compound Nd_2PtGe_3 which crystallizes in disordered AlB_2-type structure. Performed magnetic properties and specific heat measurements do not present evidence for long-range ordering in this compound, however they indicated that obtained compound is another example of cluster-glass material in R_2TX_3 family with freezing temperature $T_f \approx 3$ K.

Experimental

The polycrystalline Nd_2PtGe_3 sample was prepared by arc melting the appropriate amount of constituent elements: Nd (ingot, Alfa Aesar, purity 99.9 %), Pt (wire, Alfa Aesar, 99.95%) and Ge (lump, Onyxmet, 99.999%). The melting process was performed using arc furnace MAM-1 GmbH Edmund Bühler under inert (Zr – gettered high purity Ar) atmosphere. This procedure was repeated several times with additional flipping of the sample in order to homogenize the composition. The weight loss during the melting process found to be negligible (< 0.5 %). The room temperature X-ray diffraction experiment on the powdered sample (pXRD) was carried out using Cu K_α radiation on Bruker D2Phaser diffractometer equipped with XE-T detector. XRD patterns were analyzed by means of LeBail refinement, using the FullProf software package [16]. It was found that the stability and quality of the refinement is significantly improved by applying a maximal likelihood weighting scheme [17], instead of standard least-squares method. The magnetic properties were measured employing the PPMS device (Quantum Design) in the temperature range 2 – 300 K. The dc magnetic measurements were collected with VSM option in both the zero-field cooling mode (ZFC) and the field cooling mode (FC). The ac measurements were performed with AC Measurement System (ACMS) option. Magnetization data was collected in the frequency range 37 Hz to 10 kHz with the magnetic field amplitude $\mu_0 H_{ac} = 5$ mT. Heat capacity measurements were carried out on PPMS system using relaxation technique at constant pressure for different values of applied magnetic field (0 – 9 T). Resistivity measurements were performed using a standard four probe technique with platinum wire contacts spot-welded to the sample's surface.

Results and discussion

The room temperature pXRD pattern of the Nd_2PtGe_3 is presented in Fig. 2. The LeBail refinement confirmed a hexagonal crystal structure and denoted the lattice parameters for Nd_2PtGe_3 which are gathered in Table 1. The estimated c/a ratio is about 1, which means that this compound crystallize in a disordered variant of AlB_2–type structure and suggests the occurrence of magnetic frustration. Moreover this compound shows no superstructure lines, which were observed for ordered variant of AlB_2–type structure, Ca_2PtGe_3 [8]. Calculated lattice parameters are comparable to those reported for

Nd_2NiGe_3 [18] and Nd_2PdGe_3 [19]. It is worth to note, that the volume of unit cell increases with the increase of atomic radius of transition metal from Ni to Pt. A few weak peaks are seen in the vicinity of the (1 0 1) Bragg peak, which could not be indexed with the space group *P6/ mmm*. This trace parasitic phase was identified as $NdPtGe_2$ and cannot be removed by thermal annealing.

The temperature dependent molar magnetic susceptibility ($\chi = M/H$) of Nd_2PtGe_3 is shown in Fig. 3. The results were collected in ZFC mode for magnetic field value $\mu_0 H = 0.1$ T. It can be seen that $\chi(T)$ increases with decreasing temperature, which is typical behavior for Curie–Weiss paramagnets and may be described by the equation:

$$\chi = \chi_0 + \frac{C}{T-\theta_{CW}},$$

where C is the Curie constant, χ_0 is the temperature-independent susceptibility and θ_{CW} is the paramagnetic Curie temperature. The $1/\chi$ vs T plot (inset of Fig. 3) shows linear behavior in temperature range 20 - 300 K. Fitting the Curie-Weiss law to this region yields $\theta_{CW} = -5.17(2)$ K that suggests the presence of average antiferromagnetic interactions. The value of an effective magnetic moment (μ_{eff}) was calculated using formula:

$$\mu_{eff} = \left(\frac{3Ck_B}{\mu_B^2 N_A}\right)^{1/2}$$

where k_B - the Boltzmann constant, μ_B - the Bohr magneton and N_A - the Avogadro number. The resulting $\mu_{eff} = 3.71\ \mu_B$ in agreement with the theoretical free moment of Nd^{3+} ion ($\mu_{theo} = g_J\sqrt{J(J+1)} = 3.62\ \mu_B$ [9]).

To understand the exact nature of magnetic properties of Nd_2PtGe_3, the dc magnetic susceptibility was measured as a function of temperature both in ZFC and FC modes for various applied fields ($\mu_0 H$ = 0.01, 0.03, 0.1, 0.3 and 1 T). The results are presented in Fig. 4. It can be observed, that for low applied magnetic field, ZFC curves exhibit a wide peak with a maximum at about 3 K, which shifts to lower temperature with increasing value of $\mu_0 H$. At low temperatures $\chi_{ZFC}(T)$ and $\chi_{FC}(T)$ curves tend to diverge below a certain temperature called the temperature of irreversibility (T_{irr}). The difference between these two curves becomes negligible above the applied magnetic field value $\mu_0 H = 0.1$ T. Such type of smeared peaks in $\chi_{ZFC}(T)$ and bifurcation between $\chi_{ZFC}(T)$ and $\chi_{FC}(T)$ below T_{irr} are often observed in glassy systems due to the large distribution of cluster sizes [8, 9, 10, 11]. The inset of Fig. 4 displays plot of ZFC and FC susceptibility for external field $\mu_0 H = 0.01$ T in the lowest temperatures region. It is easy to observe that both lines merge at about $T \approx 3$ K, which in general depends on the applied magnetic field value, the size of magnetic clusters and the measuring time [3]. The precise value of this temperature was determined from a maximum of $\chi(T)$ corresponding to $d(\chi(T))/dT=0$, and is equal to $T_{irr} = 3.2$ K. This parameter is useful to calculate the empirical measure of frustration, which is defined by equation: $f = |\theta_{cw}|/T_{irr}$ and for investigated compound is equal 1.8. The obtained

value of f parameter is greater than 1, which indicates that this compound belongs to frustrated glassy systems [20].

The isothermal magnetization measurements as a function of applied magnetic field for Nd_2PtGe_3 are presented in Fig. 5. The high temperature curves change linearly as expected for a paramagnets in a Curie-Weiss regime. It is obvious that magnetization M(H) for any temperature does not saturate even at the highest applied magnetic field ($\mu_0 H$ = 9 T), which suggests absence of long-range magnetic ordering. There is no hysteresis loop in magnetic isotherms at low temperatures (T = 2 and 10 K). Moreover "S"-shape of M(H) curves suggests glassy state formation in Nd_2PtGe_3 [12], [21]. Paramagnetic behavior and a lack of magnetic ordering are also confirmed by the Arrott plot used commonly for determining Curie or Neel temperature. The $M^2(H/M)$ curves corresponding to temperatures 2, 10 and 20 K are presented in Fig. 6. From these plots it is obvious that the intercepts for all $M^2 = H/4bM - a\varepsilon/2b$ curves are negative, where a and b are parameters in Ginzburg-Landau theory and the parameter $\varepsilon=(T-T_c)T_c$. This behavior, according to mean field approach indicates occurrence of paramagnetism and a lack of magnetic ordering. In order to confirm the hypothesis about spin/cluster-glass transition in Nd_2PtGe_3, the ac magnetic susceptibility was measured at frequencies υ = 37, 117, 347, 1065, 3263 and 10 000 Hz (logarithmic spacing) with excitation field $5 \cdot 10^{-3}$ T. In order to exclude the influence of the excitation field Hac on glassy state, the measurements were performed also for a much lower field value $1 \cdot 10^{-3}$ T (not presented here). Identical results were obtained in both cases. Fig. 7 presents the real part (χ') of ac susceptibility at different frequencies measured for temperatures near T_{irr}. The $\chi'(T)$ exhibits an evident peak around 2.9 K for 37 Hz which is commonly used to determine the spin freezing temperature T_f. The T_f temperature determined from the fit to the experimental data was not very sensitive to the fit range. This characteristic temperature is slightly lower than T_{irr} and shifts toward higher temperature with increasing frequencies, which is typically considered as a signature of magnetically frustrated glassy state formation [17]. The relative shift in T_f per decade of frequency in glassy systems may be described as [10]:

$$\delta T_f = \frac{\Delta T_f}{T_f \Delta log \upsilon}$$

The calculated value of $\delta T_f = 0.014$ is one order of magnitude higher than expected for canonical spin-glass materials ($\sim 10^{-3}$), but fits well with the range that is reported for cluster-glasses (i.e. 0.028 for $Sm_2Ni_{0.87}Si_{2.87}$ [8], 0.02 for Er_2NiSi_3 [11] and 0.029 for $Nd_2Ni_{0.94}Si_{2.94}$ [10]). Another method to distinguish a cluster-glass from spin-glass system is applying the dynamical scaling theory of critical slowing down. This theory involves divergence of the correlation length at the critical temperature and can be expressed by the power law [8, 9, 10, 11]:

$$\tau = \tau_0 \left(\frac{T_f - T_{SG}}{T_{SG}} \right)^{-z\nu'}$$

where $\tau \sim 1/\upsilon$ is the relaxation time associated with measured frequency υ, zv' is dynamic critical exponent, T_{SG} is spin-glass temperature in static limit ($\upsilon \rightarrow 0$) and τ_0 is microscopic single spin flipping time. The latter one can vary from $\tau_0 = 10^{-7}$ s for cluster glass compounds to $\tau_0 = 10^{-13}$ s for spin – glass materials [3]. The values of τ_0 and zv' were estimated from linear fit of log(τ) – log(t) dependence, which is shown in the right inset of Fig. 7. The best results were received for τ_0 of the order of 10^{-8} and zv' = 3.64(2). These values indicate the cluster-glass behavior in Nd_2PtGe_3. Furthermore τ_0 is required to model spin dynamic near T_f by the empirical Vogel-Fulcher relation that is described as [1, 3]:

$$\tau = \tau_0 \, exp\left(\frac{E_a}{k_B(T_f - T_0)}\right)$$

where E_a, k_B and T_o are the activation energy, the Boltzman constant and the Vogel-Fulcher temperature, respectively. The value of the E_a/k_B ratio and T_0 have been determined from the linear fit of T_f vs $1/\ln(\upsilon_0/\upsilon)$ plot, which is displayed in the left inset of Fig. 7. Estimated values are collected in Table 2 and the E_a/k_B T_0 ratio is about 2.3 that corresponds to inter-cluster freezing process, because this parameter is usually close to 1 for canonical spin-glasses [22]. Finally the cluster-glass formation in Nd_2PtGe_3 was confirmed by Tholence criterion [23] $\delta T_{Th} = (T_f - T_0)/ T_f = 0.12$, which value is in line with our expectations. Thus, based on all ac susceptibility analysis, we suggest the cluster-glass behavior of Nd_2PtGe_3 where interacting magnetic clusters freeze below $T_f = 2.95$ K.

Different types of glassy systems are known to exhibit non-equilibrium dynamical behavior below T_f, which can be observed as the time-dependent remnant magnetization in the isothermal process [24]–[26]. We have studied magnetic relaxation phenomenon in Nd_2PtGe_3 as a final test of glassy state formation in this compound. Fig. 8 displays time evolution of magnetization measured in ZFC mode at temperatures 2 and 10 K for applied field $\mu_0 H = 0.01$ T. In ZFC protocol the sample is initially cooled down to relevant temperature without external magnetic field. After waiting for a certain time, which is necessary for temperature stabilization, a low magnetic field is applied to start recording M(t) data. It is easy to notice that for $T < T_f$ the M(t) magnetization increases even as the temperature remains constant in contrast to curve measured for $T > T_f$ which is time-independent. The experimentally observed magnetic relaxation behavior is commonly described by the well-known expression for magnetic viscosity [26]:

$$M(t) = M_0 + S\ln(t/t_0 + 1),$$

where the temperature-dependent fitting parameters M_0 and S are magnetization at t = 0 and the magnetic viscosity, respectively. The reference time t_0 depends on measuring conditions and has limited physical applicability [26]. The applicability of this formula to M(t) data collected at T= 2 K is presented as a red line in Fig. 8. Estimated values of M_0 and S are gathered in Table 2 and are comparable to results reported for other glassy systems [20] – [22].

Heat capacity (C_p) measurements with and without external magnetic field for Nd_2PtGe_3 were carried out to further investigate the character of magnetic transition. In Fig. 9 it is shown that the specific heat attains a saturation value at room temperature, which is close to classical Dulong-Petit law value: $C_p = 3nR \approx 150$ J mol^{-1} K^{-1} , where n is the number of atoms per formula unit (n = 6) and R is the gas constant (R = 8.314 J mol^{-1} K^{-1}). It is obvious that the peak observed near T = 3 K is too broad to be considered as a result of a typical long-range magnetic transition. It is reflected more clearly in the inset of Fig. 9 which exhibit low temperature dependence of C_p/T for different values of applied magnetic field ($\mu_0 H$ = 0, 1, 3, 5, 7 and 9 T). This plot shows a broad hump rather than a sharp jump generally observed in materials with long-range ordering. A well-defined upturn around T_f is strongly affected by the applied magnetic field, which can be due to glassy state formation, or alternatively, can be manifestation of a weak AFM transition in Nd_2PtGe_3. Note that the existence of strong magnetic orderings has previously been excluded by means of Arrott plot analysis.

The temperature dependent electrical resistivity of the Nd_2PtGe_3 sample in temperature range T = 2 – 300 K is shown in Fig. 10. Over the high temperature region ρ(T) weakly decreases and exhibits the expected metallic behavior without any other noteworthy features. Around T = 10 K a broad upturn can be observed, (see the inset of Fig. 10). This hump may be due to the loss of spin-disorder contribution, but the temperature at which this effect is observed disagree with heat capacity and magnetization data. This phenomenon was earlier reported in the literature [27], [28] and can be explained by that the peak in $\rho(T)$ cannot entirely be attributed to disorder in non-magnetic lattice. It was also discussed by J. Mydosh in the book [29]. As the temperature decreases further, the electrical resistivity gains the residual resistivity value ρ_0 = 1.0 μΩ m. The residual resistivity ratio is equal: $RRR = \rho_{300\ K}/\rho_{2\ K} = 1.8$, similar to observed in R_2PdGe_3 (R = Tb, Dy) [28].

Conclusions

The newly synthetized by an arc-melting process intermetallic compound Nd_2PtGe_3 crystallize in disordered variant of hexagonal AlB_2-type structure with space group P6/mmm. The structural characterization was performed by LeBail refinement of pXRD data. Calculated values of lattice parameters are equal a = 4.2455 Å and c = 4. 1933 Å which indicate that the strength of nearest-neighbor exchange (along *c*) and next-nearest-neighbor exchange (within the *ab* plane) interactions are comparable which may promote existence of magnetic frustration. The coexistent of magnetic frustration and disorder is essential to achieve a spin-glass state. The presence of glassy phase was confirmed by ac and dc magnetic susceptibility measurements. The behavior of χ_{dc} suggest presence of magnetic irreversibility at low temperatures, while measurements of χ_{ac} reveal that Nd_2PtGe_3 undergoes cluster-glass freezing behavior below T_f = 2.9 K. Moreover, this compound exhibit non-equilibrium dynamical behavior, which is typical for glassy-systems. These results are in good agreement with the heat capacity measurements, showing lack of sharp anomalies that would suggest

long-range magnetic ordering. The electrical resistivity measurements confirms metallic character of Nd_2PtGe_3.

Acknowledgments

This work was supported by Ministry of Science and Higher Education (Poland) under project 0142/DIA/2018/47 ("Diamentowy Grant").

References

[1] H. Kawamura and T. Taniguchi, "Chapter 1 - Spin Glasses," vol. 24, K. H. J. B. T.-H. of M. M. Buschow, Ed. Elsevier, 2015, pp. 1–137.

[2] D. Kaczorowski and H. Noel, "Spin-glass-like behaviour in U2TSi3(T identical to Fe, Co, Ni or Cu) intermetallics with disordered AlB2- and alpha -ThSi2-type structures," *J. Phys. Condens. Matter*, vol. 5, no. 49, pp. 9185–9195, 1993.

[3] K. Synoradzki and T. Toliński, "Effective mass enhancement and spin-glass behaviour in CeCu4MnyAl1-y compounds," *J. Phys. Condens. Matter*, vol. 24, p. 136003, Mar. 2012.

[4] T. Klimczuk *et al.*, "Cluster-glass behavior of a highly oxygen deficient perovskite, BaBi0.28Co0.72O2.2," *J. Phys. Condens. Matter*, vol. 21, no. 10, p. 105801, 2009.

[5] J. A. Mydosh, "Spin glasses: redux: an updated experimental/materials survey," *Reports Prog. Phys.*, vol. 78, no. 5, p. 52501, 2015.

[6] B. Andrzejewski *et al.*, "Magnetic Relaxation in Bismuth Ferrite Micro-Cubes," *Ferroelectrics*, vol. 448, no. 1, pp. 58–70, Jan. 2013.

[7] E. Vincent and V. Dupuis, "Spin glasses : experimental signatures and salient outcomes," Sep. 2017.

[8] T. Klimczuk *et al.*, "Crystal structure and physical properties of new Ca2TGe3 (T = Pd and Pt) germanides," *J. Solid State Chem.*, vol. 243, Aug. 2016.

[9] K. Momma and F. Izumi, "VESTA 3 for Three-Dimensional Visualization of Crystal, Volumetric and Morphology Data," *J. Appl. Crystallogr.*, vol. 44, Dec. 2011.

[10] P. Zhi-Yan, C. Chong-De, B. Xiao-Jun, S. Rui-Bo, Z. Jian-Bang, and D. Li-Bing, "Structures and physical properties of R2TX3 compounds," *Chinese Phys. B*, vol. 22, p. 56102, May 2013.

[11] S. Pakhira, C. Mazumdar, R. Ranganathan, and S. Giri, "Magnetic phase inhomogeneity in frustrated intermetallic compound Sm 2 Ni 0.87 Si 2.87," *J. Alloys Compd.*, vol. 742, Jan. 2018.

[12] S. Pakhira, C. Mazumdar, M. Avdeev, R. Bhowmik, and R. Ranganathan, "Spatially limited antiferromagnetic order in a cluster glass compound Tb2Ni0.90Si2.94," *J. Alloys Compd.*, vol.

785, May 2019.

[13] S. Pakhira, C. Mazumdar, R. Ranganathan, and S. Giri, “Chemical disorder driven reentrant spin cluster glass state formation and associated magnetocaloric properties of Nd2Ni0.94Si2.94,” *Phys. Chem. Chem. Phys.*, vol. 20, no. 10, pp. 7082–7092, 2018.

[14] S. Pakhira, C. Mazumdar, R. Ranganathan, S. Giri, and M. Avdeev, “Large magnetic cooling power involving frustrated antiferromagnetic spin-glass state in R2NiSi3 (R=Gd,Er),” *Phys. Rev. B*, vol. 94, no. 10, p. 104414, Sep. 2016.

[15] D. X. Li, S. Nimori, Y. Shiokawa, Y. Haga, E. Yamamoto, and Y. Onuki, “ac susceptibility and magnetic relaxation of ${R}_{2}{\mathrm{PdSi}}_{3}$ $(R=Nd,$ Tb, and Dy),” *Phys. Rev. B*, vol. 68, no. 1, p. 12413, 2003.

[16] J. Rodriguez-Carvajal, “Recent Advances in Magnetic Structure Determination by Neutron Powder Diffraction,” *Phys. B Condens. Matter*, vol. 192, pp. 55–69, Oct. 1993.

[17] J. Rodríquez-Carvajal and T. Roisnel, “Line Broadening Analysis Using FullProf*: Determination of Microstructural Properties,” *Mater. Sci. Forum*, vol. 443–444, pp. 123–126, 2004.

[18] S. Sarkar, D. Kalsi, S. Rayaprol, and S. Peter, “Structural and Magnetic Properties of Nd2NiGe3,” *J. Alloys Compd.*, vol. 632, May 2015.

[19] S. Majumdar and E. V Sampathkumaran, “Observation of enhanced magnetic transition temperature in Nd2PdGe3 and superconductivity in Y2PdGe3,” *Phys. Rev. B*, vol. 63, May 2001.

[20] A. P. Ramirez, “Strongly Geometrically Frustrated Magnets,” *Annu. Rev. Mater. Sci.*, vol. 24, no. 1, pp. 453–480, Aug. 1994.

[21] S. Pakhira, C. Mazumdar, and R. Ranganathan, “Low-field induced large magnetocaloric effect in Tm2Ni0.93Si2.93: Influence of short-range magnetic correlation,” *J. Phys. Condens. Matter*, vol. 29, Oct. 2017.

[22] S. Pakhira, C. Mazumdar, A. Basu, R. Ranganathan, R. N. Bhowmik, and B. Satpati, “Unusual bidirectional frequency dependence of dynamical susceptibility in hexagonal intermetallic Pr2Ni0.95Si2.95,” *Sci. Rep.*, vol. 8, no. 1, p. 14870, 2018.

[23] J.-L. Tholence, “Recent experiments about the spin-glass transition,” *Phys. B+C*, vol. 126, no. 1, pp. 157–164, 1984.

[24] H. Nair *et al.*, “Memory effect in Dy 0.5 Sr 0.5 MnO 3 single crystals,” *J. Phys. Condens. Matter*, vol. 22, p. 346002, Sep. 2010.

[25] S. Sarkar, A. Mondal, N. Giri, and R. Ray, “Spin glass like transition and exchange bias effect in Co 3 O 4 nanoparticles anchored onto graphene sheets,” *Phys. Chem. Chem. Phys.*, vol. 21, Nov. 2018.

[26] G.-H. Hu, L.-W. Li, and U. Izuru, “Pressure effect on magnetic phase transition and spin-glass-like behavior of GdCo 2 B 2,” *Chinese Phys. B*, vol. 25, p. 67501, Jun. 2016.

[27] S. Peter, S. Sarkar, S. Roy, and D. Kalsi, “Ce2PtGe3: A New Ordered Orthorhombic Superstructure in the AlB2 Family with Spin Glass Behavior,” *Inorg. Chem. Front.*, vol. 4, Oct. 2017.

[28] L. Litzbarski, T. Klimczuk, and M. Winiarski, “Synthesis, structure and physical properties of new intermetallic spin glass-like compounds RE2PdGe3 (RE = Tb and Dy),” *J. Phys. Condens. Matter*, vol. 32, Feb. 2020.

[29] J. A. Mydosh, *Spin glasses: an experimental introduction*. Taylor and Francis, 1993.

Tables

Table 1

Refined structural parameters for Nd_2PtGe_3 Numbers in parentheses are statistical uncertainties of fitted parameters

Refined Formula	Nd_2PtGe_3
Space group	*P6/mmm* (No.191)
a (Å)	4.2455(1)
c (Å)	4.1933(2)
V (Å^3)	65.789(4)
Molar mass (g mol^{-3})	701.49
Density (g cm^{-3})	5.33
Nd (1*a*)	x = y = z = 0
Pt (25%) / Ge (75%) (2*d*)	x = 1/3 y = 2/3 z = 0.5
Figures of merit:	
R_p (%)	10.7
R_{wp} (%)	15.9
R_{expt} (%)	8.03
χ^2	3.90

Table 2

Selected physical properties data for Nd_2PtGe_3 Numbers in parentheses are statistical uncertainties of fitted parameters. The total error is expected to be larger due to experimental factors (e.g. trace amounts of impurity phases).

	Nd_2PtGe_3
T_f (K)	2.9 [υ = 37 Hz]
f	1.8
E_a/k_B (K)	5.9(3)
T_0 (K)	2.61(2)
Θ_{CW} (K)	-5.17(2)
μ_{Eff} (μ_B)	3.71(9)
M_0 (emu/g) $x10^{-4}$	1.05(4)
S (emu/g) $x10^{-6}$	2.8(1)
RRR	1.8

Figures

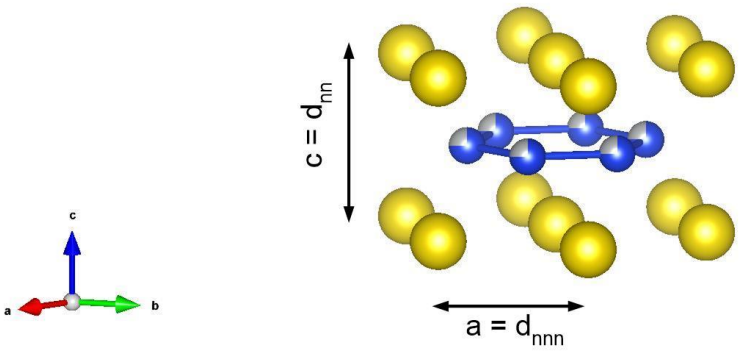

Fig. 1 Crystal structure of Nd_2PtGe_3 – big balls are neodymium, small represents platinum and germanium, which stochastically occupy hexagonal site with ratio 1:3

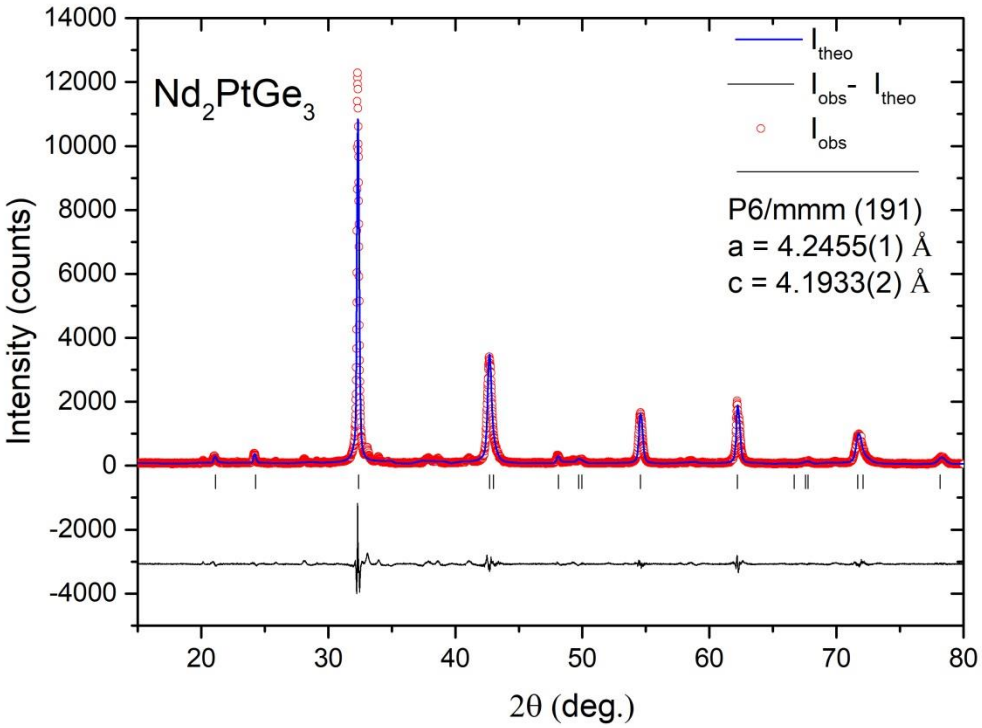

Fig. 2 Le Bail refinement of powder XRD data for Nd_2PtGe_3. Observed data and calculated intensity are represented by red circles and blue lines respectively. The difference is shown in the lower part by solid black lines. Black vertical ticks correspond to Bragg peaks for space group P6/mmm (no. 191)

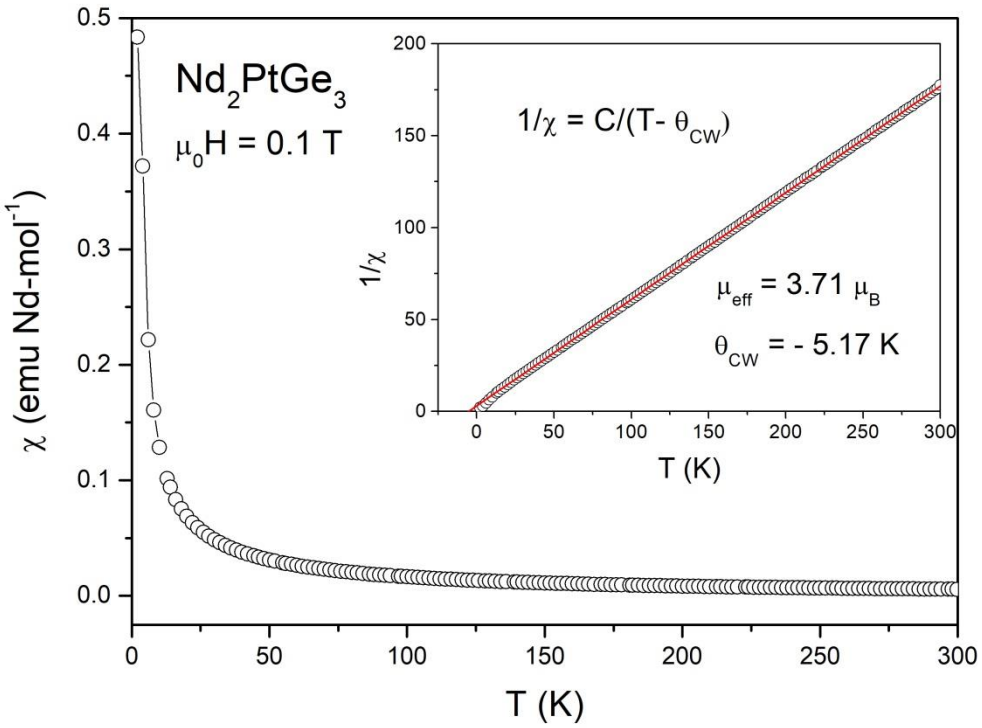

Fig. 3 The temperature dependence of the magnetic susceptibility for Nd_2PtGe_3. The inset shows inverse magnetic susceptibility in function of temperature with fitted function $1/\chi = T/C - \theta_{cw}/C$ (red line).

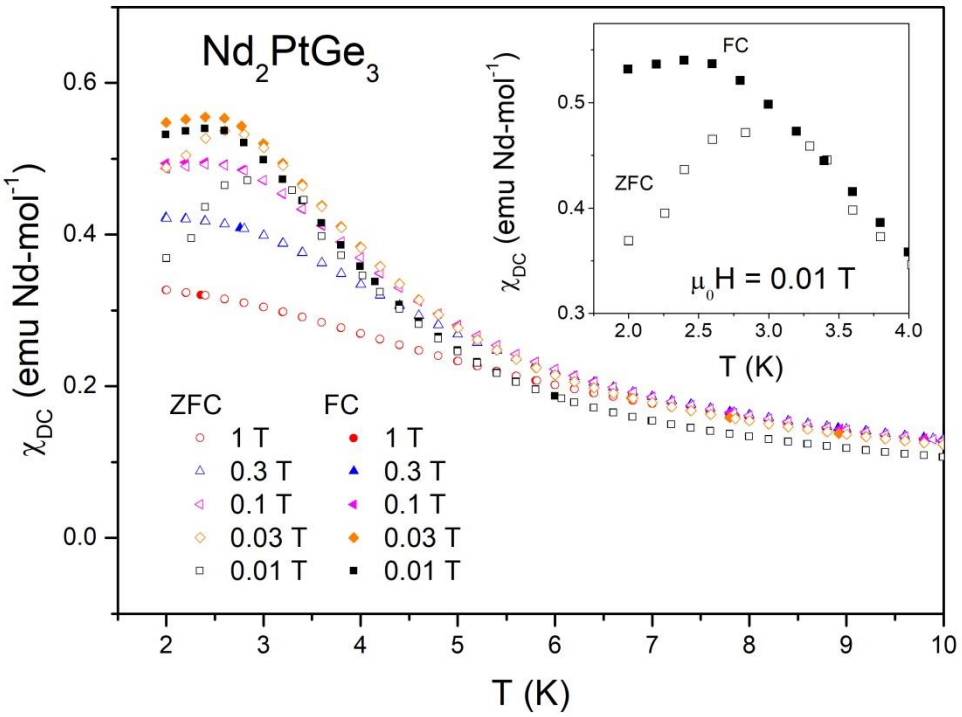

Fig. 4 The difference between ZFC and FC magnetic susceptibility of Nd_2PtGe_3 for different applied magnetic field. The inset shows the low temperature $\chi_{DC}(T)$ dependence for $\mu_0 H = 0.01$ T.

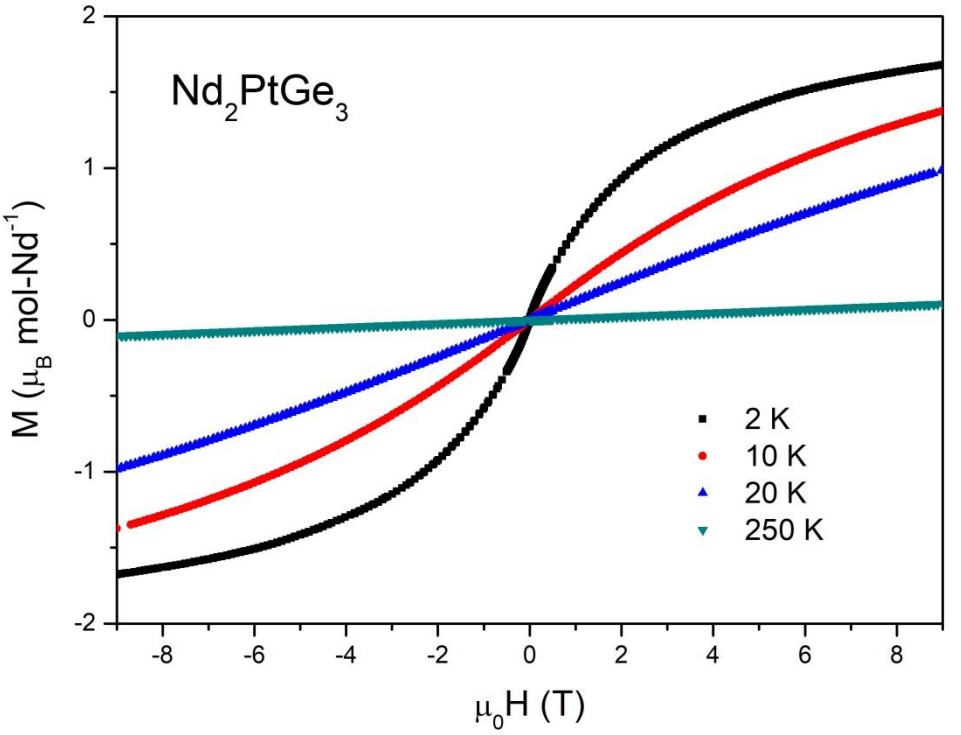

Fig. 5 Isothermal magnetization as a function of applied magnetic field of Nd_2PtGe_3 for different temperatures

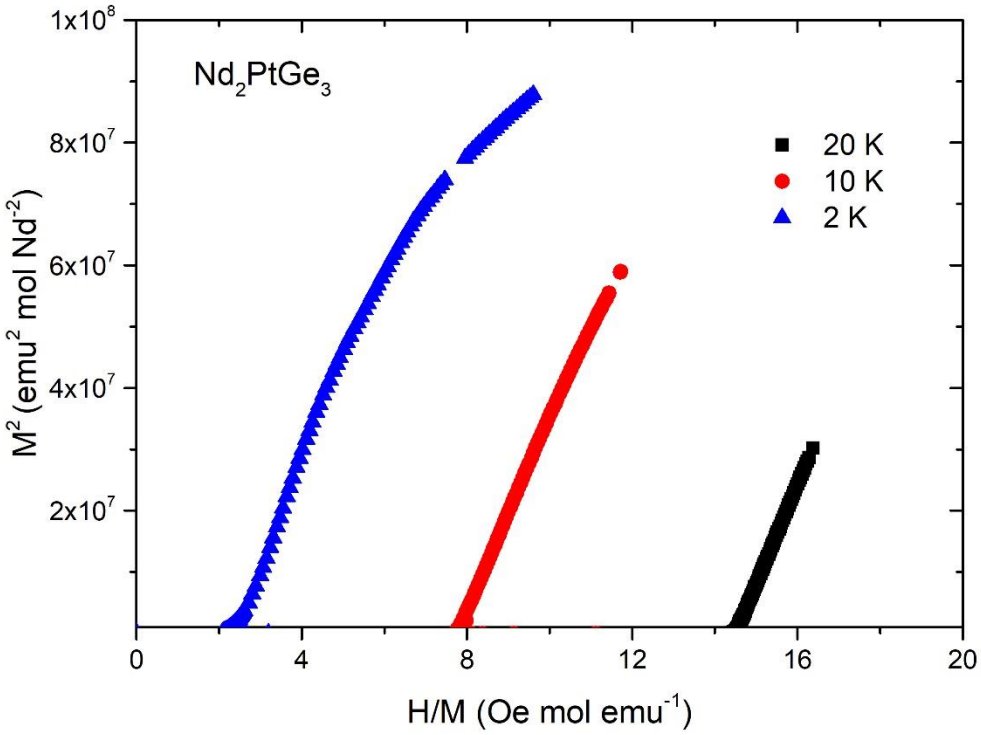

Fig. 6 Arrott plot corresponding to temperatures 2, 10 and 20 K

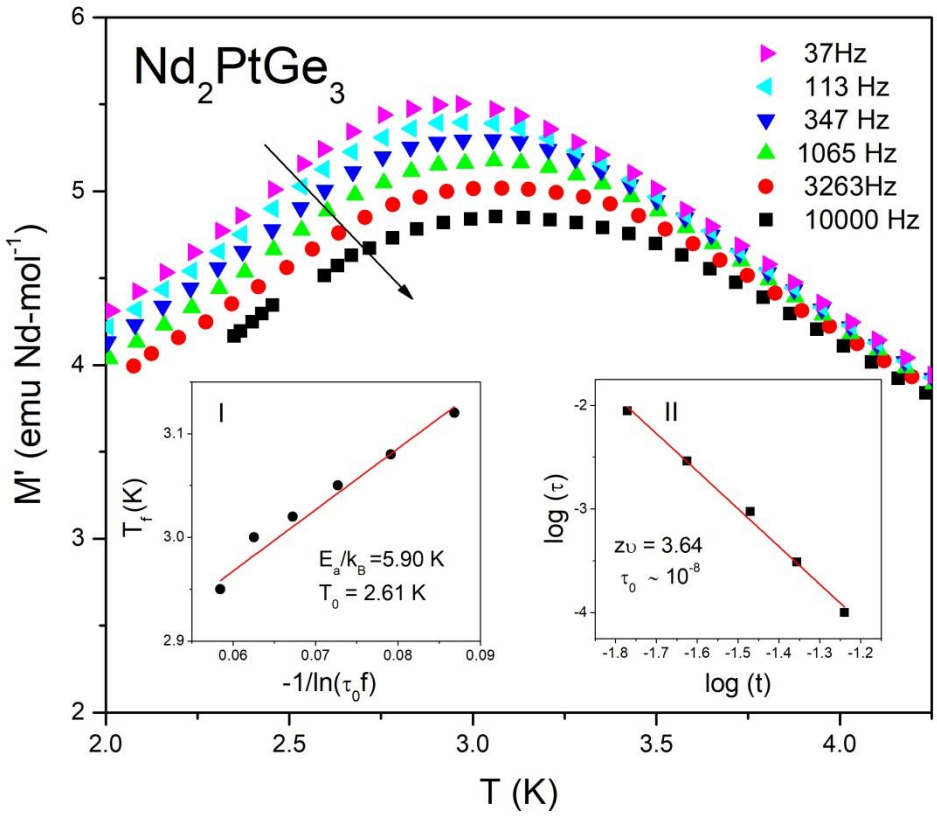

Fig. 7 Temperature dependence of the real part of the ac magnetic susceptibility χ (T) for Nd_2PtGe_3 The inset (I) shows plot of the freezing temperature (T_f) versus $1/\ln(\tau_0 f)$ with a Vogel-Fulcher law fit (red solid line). The inset(II) shows ln(τ) plotted as a function of ln(t) with the solid red line, which represents the fit to the power-law divergence.

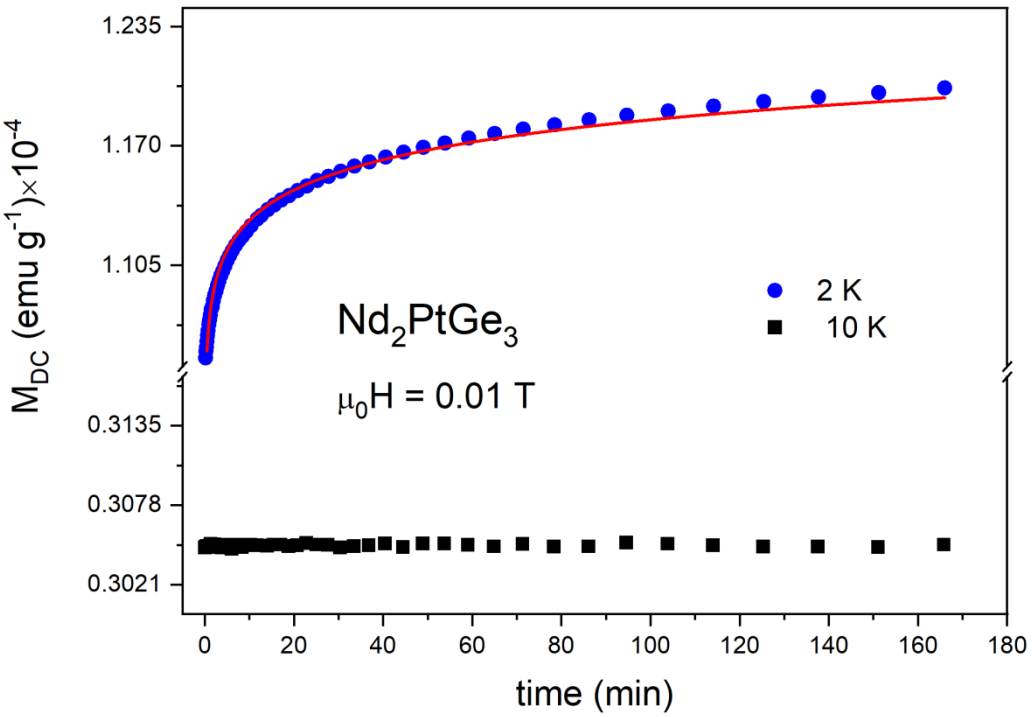

Fig. 8 Time dependent remnant magnetization behavior for Nd_2PtGe_3. Solid line represents fit to equation $M(t) = M_0 + S\ln(t/t_0 + 1)$.

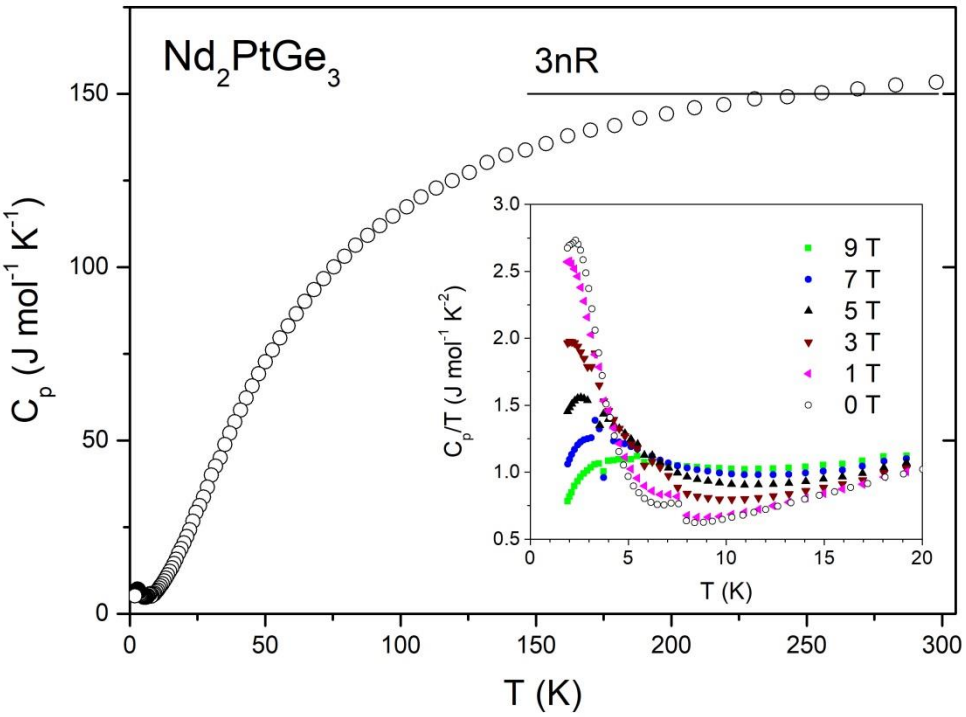

Fig. 9 Temperature dependence of the heat capacity (C_p) for Nd_2PtGe_3 The inset shows plot of C_p/T vs. T at low temperatures measured for various applied magnetic fields.

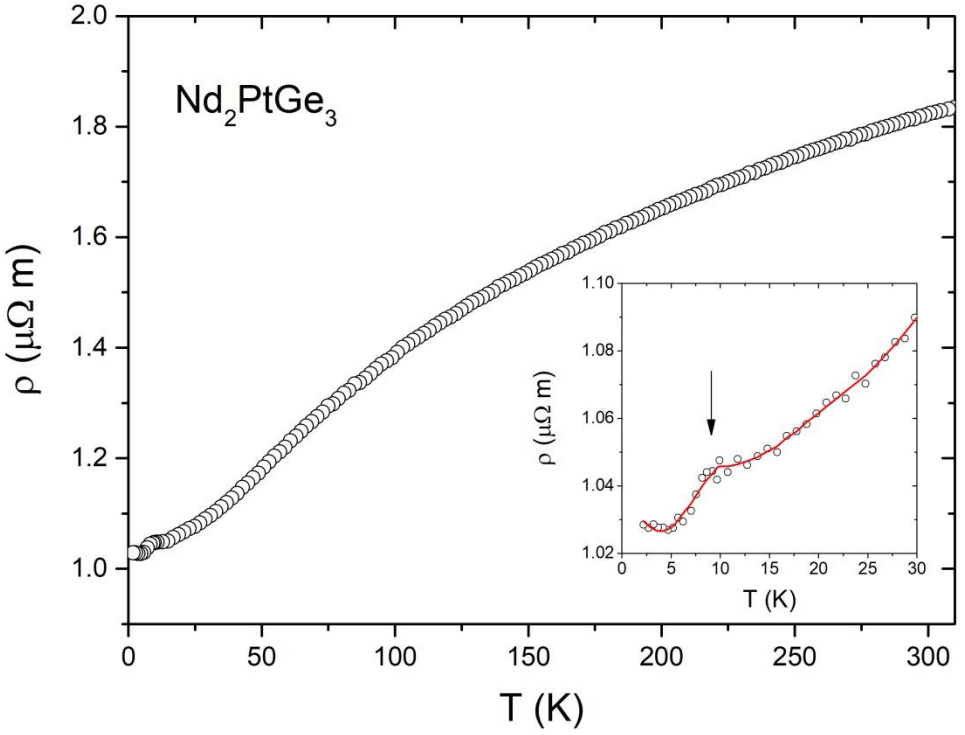

Fig. 10 Electrical resistivity for Nd_2PtGe_3 measured at zero magnetic field. The inset shows the low temperature ρ(T) dependence.